

Spectral and petrologic analyses of basaltic sands in Ka'u Desert (Hawaii) – implications for the dark dunes on Mars

Daniela Tirsch,^{1*} Robert Anthony Craddock,² Thomas Platz,³ Alessandro Maturilli,¹ Jörn Helbert¹ and Ralf Jaumann^{1,3}

¹ Institute of Planetary Research, German Aerospace Center (DLR), Berlin, Germany

² Center for Earth and Planetary Studies, National Air and Space Museum, Smithsonian Institution, Washington, DC, USA

³ Department of Geological Sciences, Freie Universität, Berlin, Germany

Received 30 May 2011; Revised 2 November 2011; Accepted 3 November 2011

*Correspondence to: Daniela Tirsch, Institute of Planetary Research, German Aerospace Center (DLR), Rutherfordstrasse 2, 12489 Berlin, Germany. E-mail: daniela.tirsch@dlr.de

ESPL

Earth Surface Processes and Landforms

ABSTRACT: Dark aeolian deposits on Mars are thought to consist of volcanic materials due to their mineral assemblages, which are common to basalts. However, the sediment source is still debated. Basaltic dunes on Earth are promising analogs for providing further insights into the assumed basaltic sand dunes on Mars. In our study we characterize basaltic dunes from the Ka'u Desert in Hawaii using optical microscopes, electron microprobe, and spectral analyses. We compare the spectra of terrestrial and Martian dune sands to determine possible origins of the Martian dark sediments. Our results show that the terrestrial sands consist primarily of medium to coarse sand-sized volcanic glass and rock fragments as well as olivine, pyroxene, and plagioclase minerals. Grain shapes range from angular to subrounded. The sample composition indicates that the material was derived from phreatomagmatic eruptions partially with additional proportions of rock fragments from local lava flows. Grain shape and size indicate the materials were transported by aeolian processes rather than by fluvial processes. Spectral analyses reveal an initial hydration of all terrestrial samples. A spectral mineralogical correlation between the terrestrial and Martian aeolian sands shows a similarity consistent with an origin from volcanic ash and lava. We suggest that the Martian deposits may contain similar abundances of volcanic glass, which has not yet been distinguished in Martian spectral data. Copyright © 2011 John Wiley & Sons, Ltd.

KEYWORDS: Mars; dunes; aeolian processes; terrestrial analogs; spectroscopy

Introduction

It has long been thought that dunes and other dark deposits on Mars are composed of fine-grained basaltic material (e.g. Edgett and Lancaster, 1993; Christensen *et al.*, 2000; Bandfield, 2002; Mangold *et al.*, 2007). It has been shown that most of the sand-sized particles seen in Lander images of the Martian surface consist of mafic and ultramafic lithic and mineral fragments (Smalley and Krinsley, 1979; Baird and Clark, 1981; Golombek *et al.*, 1997; Squyres *et al.*, 2004, 2007). The ubiquitous presence of basalt and basaltic dunes has now been confirmed by high-resolution orbital imagery (Bourke *et al.*, 2008), remote sensing observations (e.g. Fenton and Bandfield, 2003; Tirsch, 2009), and Lander data (Squyres *et al.*, 2004). Calculations of the modal mineralogy of selected Martian dunes reveal that they are composed predominately of plagioclase, high-calcium pyroxenes (HCP), low-calcium pyroxenes (LCP), olivine, and dust [cf. table 2 in Tirsch *et al.* (2011)]. Owing to this mineralogy, many authors assumed that the dark sediments on Mars have a volcanic origin (e.g. Edgett and Lancaster, 1993; Edgett and Christensen, 1994; Bandfield, 2000; Ruff and Christensen, 2002; Fenton and Bandfield, 2003; Rogers and Christensen, 2003; Wyatt *et al.*, 2003; Fenton, 2005; Hayward *et al.*, 2007; Tirsch, 2009; Tirsch *et al.*, 2011). However, the origin of the

dark aeolian sediments on Mars is still debated. Alternatively, these sediments could be the product of well-preserved impact related materials such as impact glasses or impact melts generated by impact cratering on Mars (e.g. Basilevsky *et al.*, 2000; Schultz and Mustard, 2004; Wrobel and Schultz, 2006, 2007; Moroz *et al.*, 2009).

Laboratory and remote sensing analyses of potential terrestrial analogs are useful approaches for better understanding the geological and geomorphological history of dunes on Mars. There have been a number of different approaches to better understand the nature of basaltic materials, including simulations of basaltic weathering (Bullock and Moore, 2004; Hausrath *et al.*, 2008), laboratory analyses of *in situ* basaltic alteration products (Morris *et al.*, 1990; Bell *et al.*, 1993; Golden *et al.*, 1993; Bishop *et al.*, 2007; Hamilton *et al.*, 2008), and field analog studies (Edgett and Blumberg, 1994; Baratoux *et al.*, 2007; Mangold *et al.*, 2010b). Unfortunately, there are only a few places on Earth where potential analogs to the dark Martian dunes exist, including parts of the western United States, New Zealand, Iceland, and Hawaii where volcanoclastic aeolian sediments have a provenance in basaltic host rocks (Edgett and Lancaster, 1993). The basaltic dunes in Hawaii are especially promising analogs for addressing the source of Martian dunes because of the co-occurrence of active volcanic

processes and dune development. This rare geologic setting allows the study of the entire process of dune formation from the emplacement of probable source materials to the resulting aeolian bedforms.

Laboratory analyses of Hawaii's Keanakako'i tephra (Schiffman *et al.*, 2000, 2002) indicate that palagonization occurs in response to hydrothermal alteration and is typically isolated to caldera-boundary faults. Tephra analyzes from Haleakala volcano in Hawaii indicate that unaltered tephra is composed of glass, feldspar, pyroxene, and olivine whereas alteration products include iron (Fe)-oxides, phyllosilicates, and sulfates, as well as selected area electron diffraction (SAED) amorphous aluminum-silicon (Al-Si)-bearing material (Morris *et al.*, 1990; Bell *et al.*, 1993; Golden *et al.*, 1993; Bishop *et al.*, 2007). Hamilton *et al.* (2008) collected spectra of basaltic tephra from Mauna Kea volcano that were altered under ambient, hydrothermal, and dry heat conditions. Several other recent studies have focused on the coatings that sometimes occur on Hawaiian basaltic rocks (Minitti *et al.*, 2007) in attempt to explain the high-SiO₂ component of Type 2 surfaces identified by thermal emission spectrometer (TES) data (Bandfield, 2000). Schiffman *et al.* (2006) analyzed siliceous-sulfate coatings that result from acid-fog precipitation from Kilauea in the Ka'u Desert and suggested that such a mechanism could explain the jarosite-bearing outcrops identified by the MER Landers (Squyres and Knoll, 2005; Squyres *et al.*, 2008). Analyses of airborne visible/near infrared imaging spectrometer (AVIRIS) data by Seelos *et al.* (2010) indicate that silica is present as coatings on lava flows, as a cementing agent in ash crusts, and as incrustations around active solfataras sites throughout the upper part of the Ka'u Desert.

Edgett and Lancaster (1993) noted that dunes composed of reworked volcanoclastic sediments make up a rare, but important composition class of terrestrial dunes. Edgett and Lancaster (1993) conducted field studies and an analysis of thermal infrared multispectral scanner (TIMS) data for the shifting sand dunes of Christmas Valley, Oregon. They suggest that additional infrared spectra of basaltic materials would be useful in

constraining Martian remote sensing data. More recent work on basaltic sands has been conducted in Iceland by Baratoux *et al.* (2007) and Mangold *et al.* (2010a). They show that abrasion of the local Eldborgir lava flows by aeolian-blown sand increases the amount of material available for transport. Eventually olivine is preferentially sorted and increases in abundance downwind across the sand sheet. A limitation of the Mangold *et al.* (2010b) study is that the sand source was previously modified by glacial transport. However, their results give reason to suggest that there will also be variations in the composition of the basaltic material found in the Ka'u Desert as these materials have the potential of being transported by either wind and water ~20 km to the sea. To date the only published study of the Ka'u Desert basaltic material has been presented by Gooding (1982). He concluded that the sand was derived largely from the Keanakako'i Formation and suggested that the material was too well-sorted to have been emplaced directly from a base surge (Christiansen, 1979); however, his analysis consisted of one sample collected from a sand dune along the Footprints Trail and another collected from the Keanakako'i Formation less than 1 km away.

Our study is intended to (i) characterize the basaltic sands petrologically, (ii) to determine if the dune sands originate from the stripping of Keanakako'i tephra or from local reworked tephra emplaced by larger phreatomagmatic eruptions, (iii) to determine the transport mechanisms of the material (i.e. fluvial and/or aeolian), and (iv) to assess the implications for the potential sediment sources of Martian basaltic dunes.

Geologic Setting of Ka'u Desert

Kilauea is an active basaltic shield volcano that constitutes the south-eastern portion of the Island of Hawaii. The Ka'u Desert extends over ~350 km² and is located on the western flank of Kilauea (Figure 1). The area is roughly bounded by

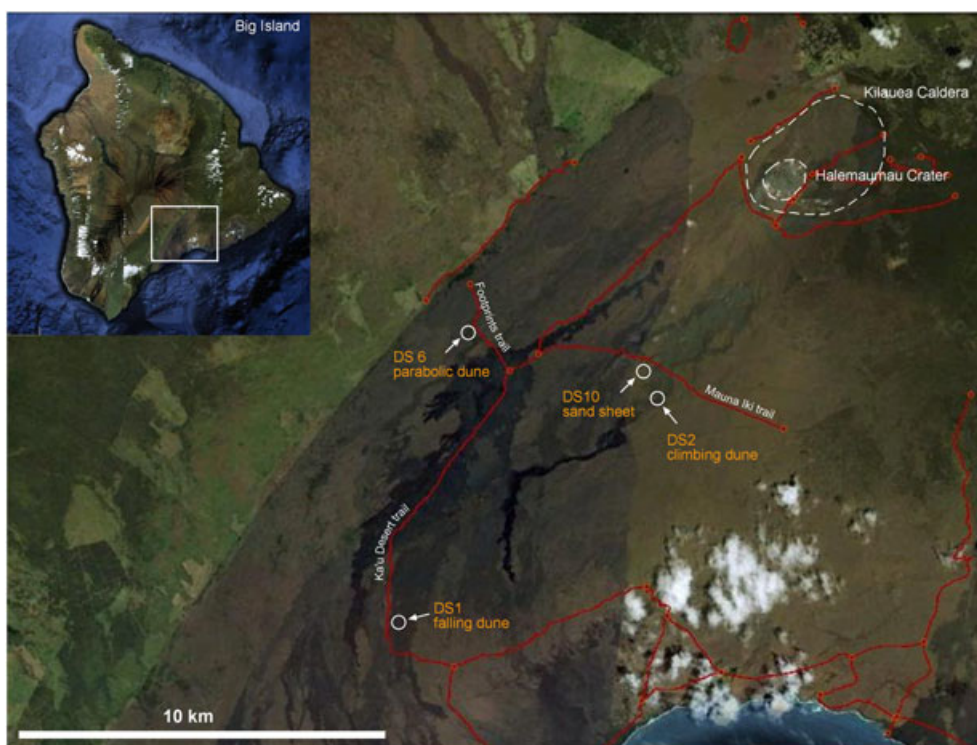


Figure 1. Context map of the study region Ka'u Desert showing the location of the sample collection sites. Top left: context map of Big Island of Hawaii. (image credit: Google Earth ©2010).

the location of Hawaii State Highway 11 to the north, the National Park Service's Hilina Pali Road to the south, Kilauea caldera to the east, and the Pacific Ocean to the west. Typically the area only receives ~130 cm of rain every year (Giambelluca and Sanderson, 1993; Juvik and Juvik, 1998), but occasionally a heavy thunderstorm (i.e. a Kona Storm) can precipitate many times this amount in a single event. Except for the effects from the low average annual rainfall, the Ka'u area also remains a desert because of toxic gasses being released from the central pit caldera, Halemaumau, and fumaroles that are concentrated along fractures near the summit of Kilauea. On average Kilauea outgases over 4.15×10^5 tons of sulfur dioxide (SO₂) every year (Elias *et al.*, 1998). The trade winds that steadily blow towards the west carry these gases into the desert creating harsh, acidic conditions that deters almost all plant life. For the purposes of our study we separated the Ka'u Desert into two broad physiographic provinces: the continuous deposit of the Keanakako'i Formation and the Ka'u Lava Ramp.

The Keanakako'i Formation

The Keanakako'i Formation is the source of all basaltic material found in the Ka'u Desert. This tephra deposit essentially includes all fragmental deposits emplaced on the rim of Kilauea by explosive eruptions. Near the summit of Kilauea the Keanakako'i Formation is more than 10 m thick (e.g. Decker and Christiansen, 1984) with a large exposure located in the Keanakako'i Crater, thus giving it its name. There are many layers within the Keanakako'i Formation that record the history of explosive eruptions at Kilauea. Basically, there are two principal units that are easily distinguishable in most exposed cross-sections. The lower unit consists of vitric ash and pumice and has a slight greenish-gold color. The upper unit consists of ash, lapilli, and lithic fragments and has a slight purplish color. Noting these distinct differences between the upper and lower units, Powers (1916) suggested phreatomagmatic eruptions at Kilauea took place during two separate periods: during prehistoric times and in 1790, as indicated by at least two older erosional surfaces (McPhie *et al.*, 1990; Mastin, 1997), particularly between the upper lithic unit and the lower vitric unit. In the 1980s the generally accepted interpretation was that the Keanakako'i Formation was emplaced entirely during the 1790 eruption (Malin *et al.*, 1983; Decker and Christiansen, 1984; Easton, 1987). The current understanding is that Kilauea has experienced periodic phreatomagmatic eruptions for at least the last 2000–3000 yr (Dzurisin *et al.*, 1995). Such eruptions are probably triggered when conditions (e.g. an offshore eruption) cause the caldera floor to sink below the water table (McPhie *et al.*, 1990; Mastin, 1997), which is located ~500 m below the surface (Stearns and MacDonald, 1946; Zablocki *et al.*, 1974). In 1924 the floor of Halema'uma'u quickly dropped to a depth of over 400 m below the surface within a period of a few weeks (Decker and Christiansen, 1984). This subsequently triggered a phreatomagmatic eruption that deposited small amounts of ash and blocks near the summit. More recently another small phreatomagmatic eruption began in March of 2008 (Wilson *et al.*, 2008).

The Ka'u Lava Ramp

The Ka'u Lava Ramp begins at the edge of the continuous deposit of the Keanakako'i Formation; however, discontinuous occurrences of the Keanakako'i extend another ~4 km west

towards Mauna Iki, a small shield volcano that erupted in the early 1970s (Malin *et al.*, 1983). The surface of the Ka'u Lava Ramp is composed primarily of weathered, prehistoric lava flows that form the western flank of Kilauea. The ramp extends from the summit to the ocean over a distance of ~20 km with a relief of ~1180 m and an average slope of ~0.04°. There is also evidence for ponding and overflow within many of the small undulations and depressions that typify the prehistoric lava flows. Sediments transported from the Keanakako'i during major flood events have infilled many of the broader, low-lying areas. Test augering has shown that the sand is over 1–1.5 m thick in places. Another important characteristic is that aeolian processes have created climbing dunes on the lee side of many topographic obstructions (Malin *et al.*, 1983). A major concentration is located on the eastern side of Cone Crater (Malin *et al.*, 1983). Many of the older aa flows have almost been completely buried by sand because their rough surfaces trap any material that is blown past. We have identified several different types of aeolian dune forms within the Ka'u Desert, including sand sheets as well as crescentic, climbing, falling, and parabolic dunes (Figure 2). The latter appear to have been barchans before the encroachment of vegetation. Obviously in an environment where both fluvial and aeolian processes occur there will be some instances where the samples we collected will show effects of both processes. However, material that formed dunes can be assumed to have been emplaced predominantly by aeolian processes. In contrast, material that is contained in channels, playas, and floodout deposits can be assumed to have been emplaced by fluvial processes.

Dark Dunes on Mars

There are numerous dark dunes deposited on impact crater floors on Mars. For the comparison with terrestrial basaltic sand dunes we selected three dunefields, which represent the majority of the Martian deposits spectrally, morphologically, and physically. The geographical locations of the selected dark aeolian deposits on Mars and their nearest volcanic regions are shown in Figure 3.

The dunefield in Moreux crater (Figure 4A) consists of bachanoid dunes associated with barchans and sand sheets. The crater is located at the highland/lowland boundary nearby Protonilus Mensae, at a distance of 2226 km from the next volcanic edifice Nili Patera at Syrtis Major (see Figure 3). The modal mineralogy of this dunefield indicates both high-calcium pyroxene (HCP) and low-calcium pyroxene (LCP) (HCP = 25 vol.%, LCP = 10 vol.%) and olivine (7 vol.%) in a mixture with plagioclase (55 vol.%) and dust (3 vol.%) (Tirsch *et al.*, 2011). Calculations of the thermal inertia and estimations of the grain size yield medium sand in the range of 385 µm (Tirsch, 2009). See Figure 5 for a diagram illustrating the mean grain sizes of all samples analyzed here.

A further selected dark dunefield is located on the floor of an unnamed crater located in Tyrrhena Terra (Figure 4B) at a distance of about 740 km from Tyrrhena Patera, the closest volcanic region (see Figure 3). The dunefield consists exclusively of barchan dunes and the thermal inertia of the deposit indicates a grain size of 360 µm (medium sand). The modal mineralogy of this deposit is 17 vol.% HCP, 7 vol.% LCP, 10 vol.% olivine 56 vol.% plagioclase and 10 vol.% dust (Tirsch *et al.*, 2011).

Reuyl crater (Figure 4C) is located close to the volcano Apollinaris Patera (410 km distance, see Figure 3). Its dark aeolian deposit comprises dunes of unclassified shapes in association with a sand sheet. The grains size is estimated to range from coarse to very coarse sand (~900 µm). Tirsch *et al.* (2011) specified the modal mineralogy of this deposit as 22 vol.% HCP, 14 vol.% LCP, 10 vol.% olivine, 51 vol.% plagioclase and 5 vol.% dust.

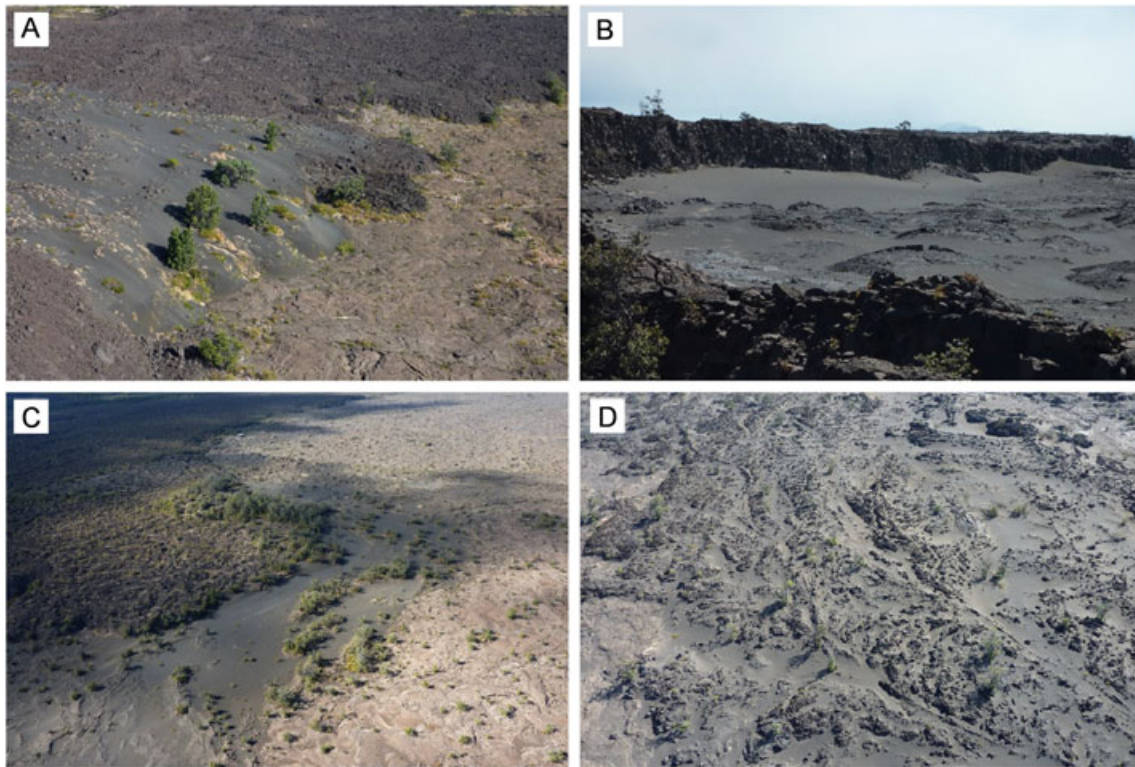


Figure 2. Basaltic aeolian bedforms in Ka'u Desert. (A) Aerial photograph of a falling dune located off the Footprints Trail. (B) Climbing dune located at the base of Kalanaokuaiki Pali along the Mauna Iki Trail. (C) Aerial photograph of a vegetated parabolic dune located off the Ka'u Desert Trail. (D) Aerial photograph of a sand sheet trapped within an aa lava flow.

Methods

Sampling and fieldwork

Different samples of aeolian material were collected during a field trip to Ka'u Desert in August 2009. Figure 1 shows the study region and the position of the aeolian bedforms analyzed. Three different dark basaltic dunes and one sand sheet were sampled.

Sample DS1 was collected from the surface of a falling dune located off the Ka'u Desert Trail, in a distance of ~17.4 km from Halemaumau/Kilauea (Figure 2A, $19^{\circ}19'29''$ N, $155^{\circ}21'51.15''$ W). This dune is about 3 m high and is sparsely vegetated. We observed saltating sand grains and ripples, which indicate active sand transport on the dune's surface. The bedform is connected to a vast sand sheet located upwind to the northeast. We assume that this sand sheet represents the local sediment source of the dune. However, the source of the sand sheet

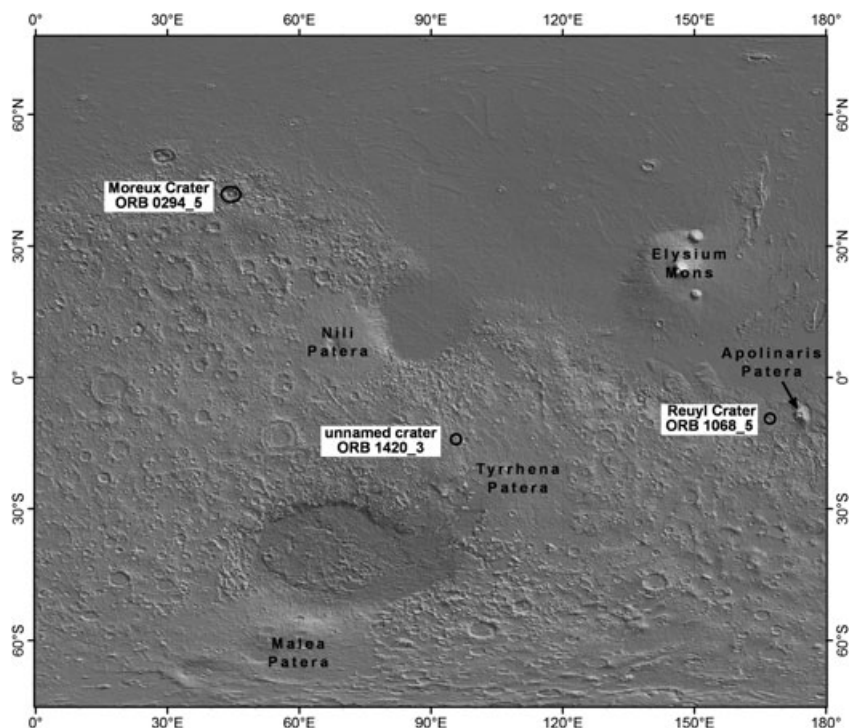


Figure 3. Location of dark aeolian deposits on Mars selected for the comparison with terrestrial basaltic dunes.

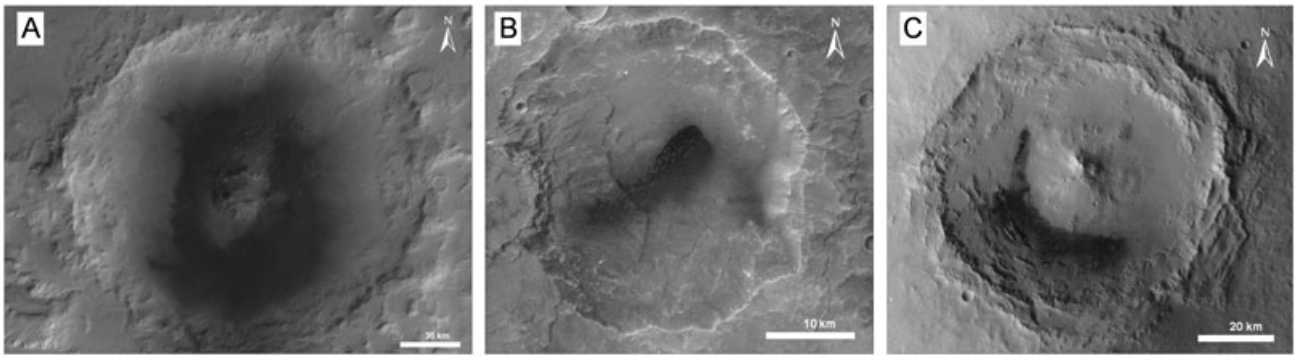


Figure 4. Dark dunefields in Martian craters selected for comparison with terrestrial basaltic dunes. (A) Dunefield in Moreux crater (42.12° N; 44.51° E). (B) Barchan dunefield in an unnamed crater at Terra Tyrrhena (14.20° S; 95.79° W). (C) Dunefield in Reuyl crater near Apollinaris Mons (9.76° S; 166.9° W).

material has not yet been determined. The aeolian sediments in this region are transported by the prevailing winds in the south to southwest direction and seem to be trapped on a rough aa flow surface. Nearly sand free older pahoehoe flows form a sharp boundary on both sides of the sand sheet. The falling dune itself is bordered by two aa flows.

DS2 and DS3 were collected from a 500 m wide and up to 7 m high climbing dune located along Kalanaokuaiki Pali nearby the Mauna Iki Trail, about 7.2 km away from Kilauea (Figure 2B, 19°20'39.43" N, 155°18'26.56" W). Its surface layer is composed of coarse sands that often build ripples with sharp crests on the dune surface. Saltating and rolling sand grains and the unvegetated nature of the dune indicate that the bedform is still active. Augering reveals that bedding is well developed throughout most of this deposit, suggesting that it has aggraded over time from aeolian activity. The top coarse sandy portion is interbedded by a thin (2–4 cm) layer of clay-rich material. It may represent a weathered ash layer that was either emplaced during an eruptive event or potentially washed over the dune from surrounding clay-rich material during a period of quiescent. Below 2.1 m depth the dune is composed of vitric-rich sand. Our analyses show that many of these particles are fragile glass shards. Both main units within the dune correspond to the general stratigraphy recognized in the Keanakako'i tephra (Mastin, 1997). DS2 was taken from the dune surface and DS3 represents a layer at 2.9 m depth.

DS6 was collected from a large parabolic dune located off the Footprints Trail, in a distance of ~10.3 km from Kilauea (Figure 2C, 19°21'17.52" N, 155°21'51.59" W). This bedform is heavily overgrown by trees and bushes indicating inactivity and a considerable time lapse following deposition. Originally, it might have been a barchan dune prior to the encroachment of vegetation. However, some unvegetated parts of the dune show coarse-grained ripples, pointing to recent sand transport in certain areas. The deposit is bordered to the southwest by an aa flow and several smaller sand sheets deposited on prehistoric pahoehoe flows to the northeast.

DS10 was collected from a small isolated sand sheet located near the Mauna Iki Trail, about 6.2 km from Kilauea (Figure 2D, 19°21'3.00" N, 155°18'19.14" W). The sand of this deposit was trapped on a rough aa flow which is still visible within the sheet. Active sand transport is observed on smoother areas based on saltating sand grains and the formation of ripples.

Microscope and electron microprobe analyses

A split of each sample was taken to prepare grain mounts and polished thin sections for both microscopic and electron microprobe (EMP) analyses. A polarizing microscope with a micrometer scale was used to determine grain size, shape, and componentry. The thin sections were carbon-coated and individual minerals and glass shards selected for EMP analysis were measured.

For the analysis of glass and minerals we used a JEOL JXA 8200 superprobe at Freie Universität Berlin. It is equipped with five crystal spectrometers (wavelength dispersive spectrometer, WDS) for elements beyond carbon (Z=6) and one energy dispersive X-ray detector (energy-dispersive X-ray spectrometer, EDS) for elements beyond sodium (Z=11). Mineral analyses were carried out with a focused beam whereas for glass analyses a defocused beam (diameter approximately 20 μm) was applied to minimize the loss of sodium and potassium (Froggatt, 1983). For both mineral and glass analyses a voltage of 20 kV was used. Glass EMP analyses were checked for contamination following the procedure described by Platz *et al.* (2007). Those analyses that showed contamination by a mineral phase (primarily by plagioclase microlites) were removed from the dataset.

Spectral analyses

The visible/near-infrared (VIS/NIR) reflectance spectra of the dune sand samples (DS1, DS2, DS3, DS6, DS10) were acquired relative to Spectralon (holding 95% reflection) under ambient conditions from 0.5 to 2.5 μm at the GFZ German Research

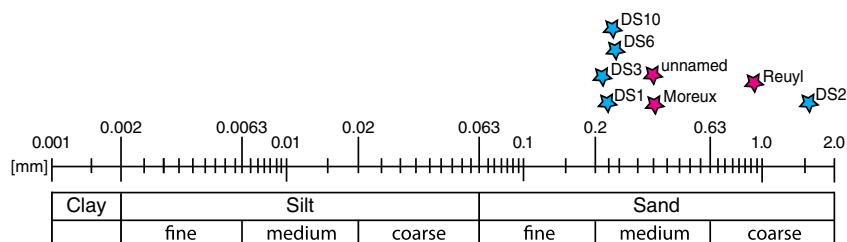


Figure 5. Illustration of mean grain sizes for Ka’u Desert and Martian sand samples. This figure is available in colour online at wileyonlinelibrary.com/journal/esppl

Center for Geosciences by using an analytical spectral device (ASD) FieldSpec Pro spectrometer. Except for drying (air dried in the laboratory), no special sample preparation was performed. For each sample we took 10 reflection spectra from 0.5 to 2.5 μm each consisting of 50 single scans. In between the individual measurements the beam was slightly shifted over the sample in order to gain a representative spectrum of the sample. From these single measurements we created an average spectrum, which best reflects the mineralogical composition. For the coarse-grained sample DS2, a bidirectional measurement was performed in order to avoid shadow effects.

In addition, further reflectance spectra were acquired at the Planetary Emissivity Laboratory (PEL) (Maturilli, 2010) located at the DLR Institute of Planetary Research. We used a Bruker IFS 88 Fourier-transform infrared (FT-IR) spectrometer equipped with a Harrick Seagull™ reflectance accessory for the VIS/NIR spectral range from 0.4 to 1.2 μm . The near-infrared measurements from 1.2 to 2.5 μm were obtained by means of a Bruker Vertex 80V FT-IR spectrometer, which can be operated under vacuum conditions to remove atmospheric noise from the spectra. The Vertex 80V is evacuated at 1 mbar pressure in room air purged of carbon dioxide (CO_2) and water (H_2O). The samples are kept under both purging and vacuum for 10 minutes before measuring the reflectance, to stabilize the ambient conditions. However, before the measurements, the samples are kept several hours in the desiccators at stable temperature and low-controlled humidity. This additional spectroscopic analysis was performed in order to compare the differences between the measurements under ambient and vacuum conditions and to reveal possible atmospheric effects on the spectra.

Results

Petrology

Microscope analyses revealed a high amount of volcanic glass fragments in the sand samples, with subsidiary amounts of feldspars, olivine, and pyroxene (Table I). Figure 6 provides

an impression of the different particles proportions in the samples set.

Sample DS1 (falling dune) material is of medium sand grain size and has a dark gray to black color. It contains volcanic glass shards, clinopyroxene, feldspar, olivine, and rock fragments. Some glass shards are altered and recrystallized. The shapes of the mineral grains range from angular to subrounded (Table I). Sample DS2 (climbing dune, top layer) is much coarser-grained than any other studied samples. It is composed mainly of rock fragments. Large subrounded olivine grains are easily visible to the unaided eye. Thin sections show minor abundances of clinopyroxenes and feldspars. Glass particles are predominantly dense (i.e. only minor amounts of vesicles and cavities) and are irregular in shape. Some recrystallized glasses comprise xenomorph minerals. The greenish sample DS3 (climbing dune, layer at 2.9 m depth) consists of fine-grained, vitric material. The glass shards are dense to vesicular and have an angular shape. The sample is composed of glass shards with traces (< 1 vol.%) of olivine and feldspar (Table I). Sample DS6 (parabolic dune) contains angular, fine to medium sand particles. The dense to vesicular glass shards appear relative fresh. Minor components (< 10 vol.%) of the sample comprise lithic fragments, olivine, and clinopyroxene (Table I). Sample DS10 (dark ripple) contains medium sand, subangular to subrounded particles. Glass fragments, that embody ~50 vol.% of the sample, show different degrees of alteration. About 90 vol.% of the glass fraction consists of fresh light to dark brown glass with the remaining portion showing minor to moderate alteration. Rock fragments represent about 40 vol.% of the total sample whereas the constitutes of olivine, clinopyroxene, and feldspars represent the remaining 10 vol.% (Table I).

Microprobe analyses were used to determine the mineral and glass geochemistry (see Table II). Those results are essential to cross-check the interpretation of the spectra (e.g. HCP versus LCP) and to determine the initiators of the individual absorption bands. All glass analyses show bulk silica contents between 49–50 wt.%. Based on silicon oxide (SiO_2) and alkali abundances, glass compositions are classified as basaltic. The difference of the sum of oxides to 100 is often attributed to dissolved

Table I. Petrologic analysis of Ka'u Desert sand samples.

Sample ID	Location	Content	Grain shape	Comments
DS1	Falling dune	Glass	Subrounded	Mainly glass shards
		Olivine	Angular to subangular	Some recrystallized glasses
		Clinopyroxene	Angular to subangular	Few single mineral grains
		Feldspar	Angular to subangular	
		Rock fragments	Subrounded	
DS2	Climbing dune (top layer)	Micas?	Subrounded	
		Glass	Subrounded	Mainly rock fragments
		Olivine	Subrounded	Glasses dense to highly vesicular
		Clinopyroxene	Subrounded	Melt intrusions in mineral phases
		Feldspar	Subrounded	Partially recrystallized glasses
DS3	Climbing dune (vitric layer at 2.9 m)	Rock fragments	Angular to subangular	Xenomorph minerals (xenocrysts)
		Glass (99 vol.%)	Angular	Glasses dense to vesicular
		Olivine	Subrounded	Bubble wall shards
DS6	Parabolic dune	Feldspar	Subrounded	Material less fresh
		Glass	Subangular	Vesicular glasses, some dense
		Olivine	Subangular	Relative fresh material
DS10	Dark ripple	Clinopyroxene	Subangular	Higher amount of mineral fragments (5–7 vol.%)
		Rock fragments (2 vol.%)	Subangular to subrounded	
		glass (50 vol.%)	Subangular to subrounded	Many crystalline fragments
		Olivine	Subrounded	Some altered glasses
		Clinopyroxene	Subangular to subrounded	Higher amount of minerals (10 vol.%)
		Feldspar	Subangular to subrounded	Fresh glass light beige to dark brown
		Rock fragments (40 vol.%)	Subrounded	

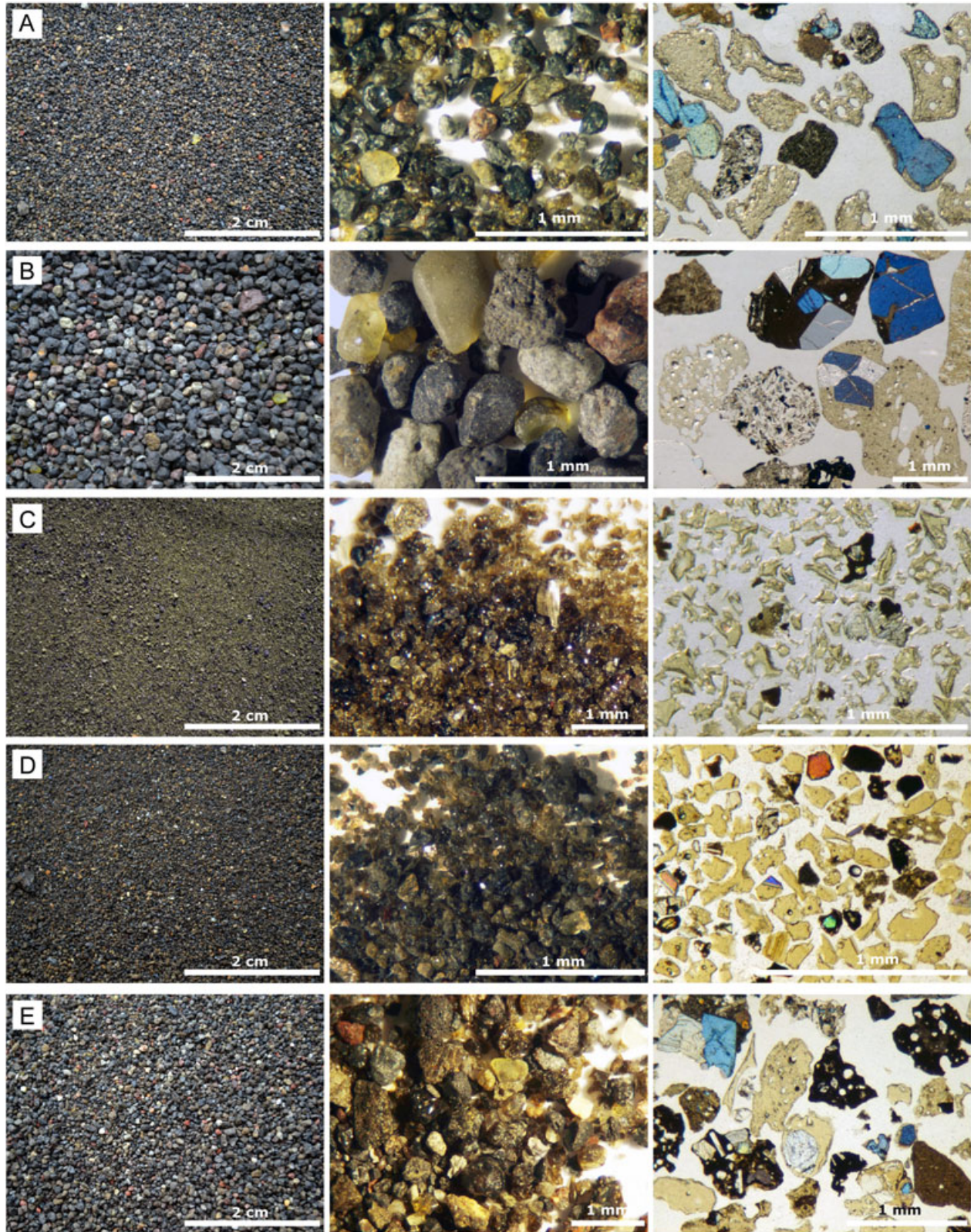


Figure 6. Photograph (left) and microscopic view (middle) of the sand samples with the corresponding thin sections (right). (A) Sample DS1 collected from the falling dune (cf. Figure 2A) dominated by glass shards and mineral grains. (B) Sample DS2 collected from the climbing dune (cf. Figure 2B) (top layer) dominated by rock fragments. (C) Sample DS3 collected from the same climbing dune (cf. Figure 2B) (vitric layer) dominated by glass shards. (D) Sample DS6 collected from the vegetated parabolic dune (cf. Figure 2C) dominated by glasses and mineral crystals. (E) Sample DS10 collected from a dark ripple (cf. Figure 2D) dominated by volcanic glass and rock fragments.

volatiles (primarily H₂O with/without minor abundances of CO₂, SO₂ etc.) in the glass which cannot be measured with an EMP. To a first-order-approximation, this difference from 100 is equal to the bulk water content either dissolved in the melt or adsorbed through hydration. According to EMP analyses several wt.% of H₂O are present in the samples (Table II).

Olivine mineral compositions are homogenous with forsterite contents of 0.84 to 0.88. Analyzed clinopyroxene crystals are classified as augites, i.e. HCPs (Morimoto, 1989). Plagioclase crystals with anorthite contents of 0.53 to 0.70 were primarily measured to check glass analyses for contamination with feldspar microlites. Our EMP analyses of glass and olivine show

deviations of up to 1 wt.% for major elements compared to results of Gooding (1982). This may be attributed to a different analytical procedure. Gooding (1982) used a 10- μm diameter beam whereas as we used a focussed, c. 1- μm diameter beam for mineral analyses and a defocused c. 20- μm diameter beam for glass.

Spectroscopy

Reflectance spectra of the samples collected in Ka'u Desert are shown in Figure 7 for measurements at ambient (Figures 7A and 7B) and vacuum (Figures 7C and 7D) conditions. Measured under ambient conditions all spectra exhibit a deep broad absorption band at 1.0 μm and narrow bands at 1.9 and 2.21 μm that vary in intensity and spectral character. The absorption at 1.0 μm is related to ferrous iron (Burns, 1993) in the samples and is suggestive of the iron-bearing minerals olivine (Sunshine and Pieters, 1998) and pyroxene (Cloutis and Gaffey, 1991), basaltic glass (e.g. Minitti *et al.*, 2002) and also some ferric oxides/oxyhydroxides (e.g. Morris *et al.*, 1985). The typical second broad pyroxene absorption band around 2 μm is less distinct in Figures 7A and 7C and seems to be overlapped by other features. However, the continuum removed spectra in Figures 7B and 7D emphasize these bands in all cases. Moreover, Figure 7B reveals further absorption bands at 1.9 μm , particularly in samples DS2 and DS10, which are indicative of molecular water (Clark *et al.*, 1990). A second narrow band in all spectra at 2.21 μm is related to bending metal-OH-bonds (Clark *et al.*, 1990). These bands almost disappear in the spectra measured under vacuum conditions (Figures 7C and 7D). This indicates that the 1.9- and 2.21- μm bands seen in Figures 7A and 7B are caused

by atmospheric moisture. Solely samples DS2 and DS10 show slight indications for hydration because these features are extremely weak but still present, often in the form of shoulders. Generally the metal-OH-bands near 2.2–2.3 μm do not change band strength with changing relative humidity conditions (e.g. Bishop *et al.*, 1994; Bishop and Pieters, 1995; Bishop *et al.*, 1995). However, some amorphous materials similar to opal and allophane do appear to exhibit decreases in the \sim 2.2 μm band strength with decreasing relative humidity. This is likely due to H-bonding of the metal-OH-bonds to adsorbed H_2O molecules (e.g. Anderson and Wickersheim, 1964; Milliken *et al.*, 2008). In summary, the strong reduction of the bands in the dried samples DS1, DS3, and DS6 measured under vacuum conditions indicates that the bands in Figure 7 are mainly due to atmospheric water whereas samples DS2 and DS10 show indications for hydration..

A comparison between Martian and terrestrial sand spectra is shown in Figure 8. The three exemplary Martian OMEGA spectra, taken from the dune fields described earlier (see Figure 4), reflect the basaltic composition of the dark dunes as typically inferred for Martian dunes (cf. Tirsch *et al.*, 2008). The spectra show a deep broad absorption band at 1 μm and a shallower broad band around 2 μm . Both bands are caused by Fe^{2+} in the minerals and are indicative of a mixture of olivine and pyroxene. The center of the 1- μm band shifts to shorter wavelengths with increasing pyroxene content for pyroxene-olivine mixtures (Cloutis *et al.*, 1986) as observed in the spectrum of Moreux crater (OMEGA orbit ORB0294_5, Figure 8). The Ka'u Desert spectra show a similar 1- μm absorption, whereas the 2- μm absorption is only visible once the continuum has been removed as shown in the insets of Figure 8. The main difference between the Ka'u Desert and the Martian spectra is the

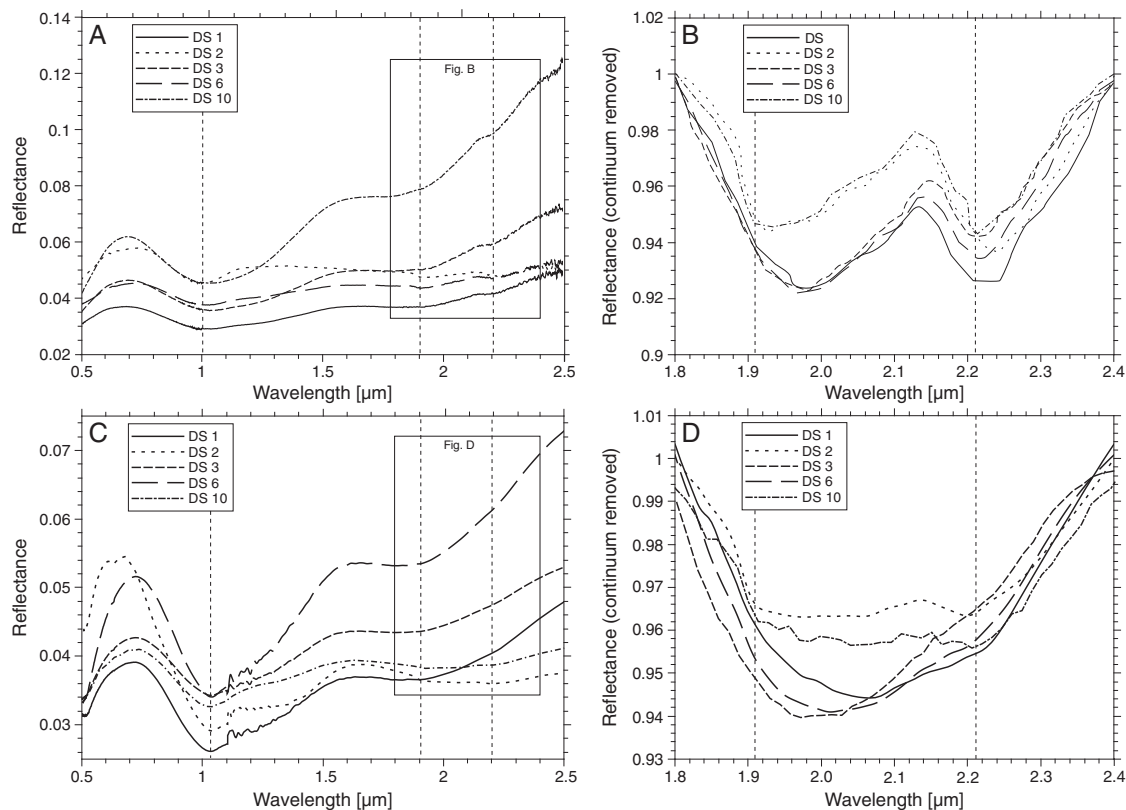


Figure 7. Reflectance spectra of the basaltic sand samples. (A) Spectra of samples DS1, DS2, DS3, DS6, and DS10 measured with the ASD spectrometer under ambient conditions. (B) Same spectra as in Figure 7A in the spectral range 1.8 to 2.4 μm with continuum removed display emphasizing the broad 2- μm band and the 2.21- μm absorptions. (C) Spectra of samples DS1, DS2, DS3, DS6, and DS10 measured in the PEL under vacuum conditions. (D) Same spectra as Figure 7C in the spectral range 1.8 to 2.4 μm with continuum removed display emphasizing the broad 2 μm band and the 2.21 μm absorptions. See text for discussion.

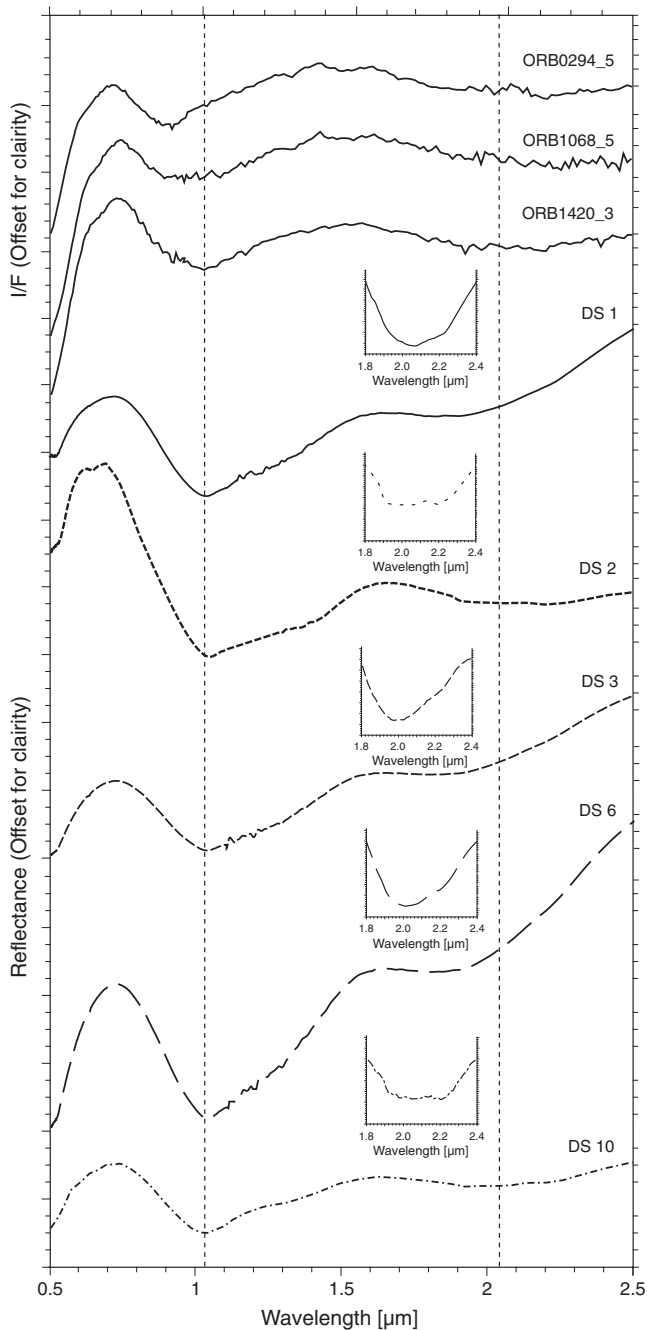


Figure 8. Comparison of Martian [OMEGA spectra: ORB0294_5 (Moreux crater), ORB1068_5 (Reuyl crater), ORB1420_3 (unnamed crater)] and terrestrial (PEL: DS1, DS2, DS3, DS6, DS10) reflectance spectra of dark dune sands. Olivine and pyroxene are represented in all spectra by the broad 1- and 2- μm bands. The insets show the broad 2- μm bands and, particularly for sample DS2 and DS10, shallower hydration bands at 1.9 and 2.21 μm in continuum removed views.

presence of the H_2O and OH associated bands at 1.9 and 2.21 μm in the spectra of the Hawaiian samples.

We compared the spectra of our samples with library spectra of high-calcium pyroxene, olivine, and iddingsite (Figure 9). The latter is a common alteration product of olivine on Earth, comprising phyllosilicates, iron oxides, quartz, and calcite (Cloutis, 2004; Orofino *et al.*, 2006). This library spectrum represents a sample that is in its initial alteration state, as indicated by the lack of the 1.4- μm band and the weakness of the 1.9- μm water-related absorption band (Orofino *et al.*, 2006). However, it represents a good intermediate stage between unaltered and altered olivine-rich material. A further example of altered olivine is shown in Figure 10A, resembling the spectral shape of our Hawaiian samples (Figure 10B).

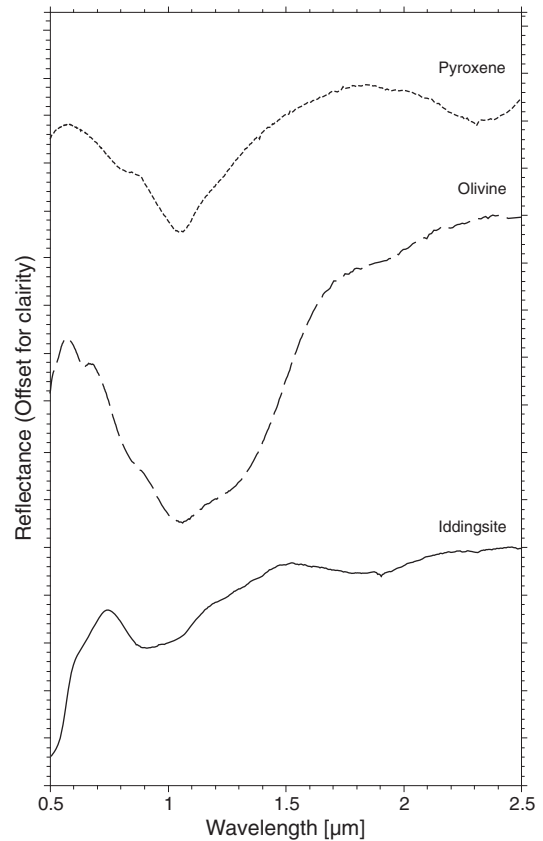


Figure 9. Library spectra of high-calcium pyroxene (HCP), olivine, and iddingsite (from US Geological Survey and RELAB spectral database) for comparison with terrestrial and Martian spectra (cf. Figure 8, see text for discussion).

Discussion

The grain shape analysis was intended to shed light on the transport mechanisms of the material. Because of its deposition as aeolian bedforms, we suppose most of the material to be aeolian transported. However, fluvial channels in Ka'u Desert give reason to suppose the involvement of fluvial processes in that region. On Earth the shape of aeolian dune material has been analyzed by many authors (e.g. Folk, 1978; Goudie and Watson, 1981; Pye and Tsoar, 1990; Chakroun *et al.*, 2009). It is well-known that terrestrial quartz grains that have been transported by aeolian processes are usually of subangular to subrounded shape. The angularity can increase with decreasing grains size (Goudie and Watson, 1981) because the impact energy released in collisions is much smaller. Since the hardness of quartz grains (Mohs scale 6.5–7) is comparable to the hardness of olivine (Mohs scale 7) and clinopyroxene (Mohs scale 6), we assume that aeolian transportation of basaltic sand grains may result in a similar subrounded to subangular grain shape. This assumption is confirmed by the results of Krinsley *et al.* (1979) who studied abrasion textures of quartz and basaltic sand under terrestrial and Martian conditions. Krinsley *et al.* (1979) concluded that mechanical aeolian abrasion of basaltic sands yield similar surface features compared to quartz grains. However, their analysis revealed that aeolian abrasion under Martian atmospheric pressures results in more rounded grains, which is attributed to the thinner atmosphere and the lower cushioning effect of the air. According to our microscope analysis, most of the samples are dominated by subrounded particles followed by subangular grains (cf. Table I). As discussed earlier, these grain shapes are usually generated by saltation and rolling during aeolian transport. These transport processes have also been observed during our field campaign. The angular shape of the glass shards

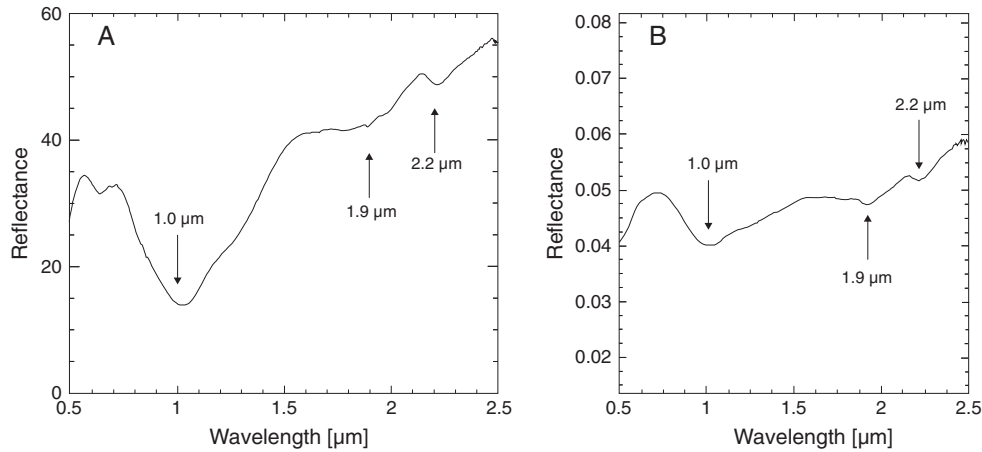


Figure 10. Spectral comparison of (A) altered olivine (grain size 106–200 μm) collected in the volcanic region Eifel, Germany (image adopted from Orofino *et al.*, 2006) and (B) sample DS10 of a dark ripple collected in Ka'u Desert. Note the correlation of absorption bands.

in sample DS3 indicates that these particles did not experience aeolian transport but seem to be rather deposited *in situ* from an eruption column (cf. Craddock *et al.*, 2010). The bubble-wall glass shards in that sample indicate that fragmentation and attrition took place before the material was deposited (Fisher, 1963). Fisher (1963) observed bubble-wall texture on abraded olivine grains of Puu Mahana Beach (Lanai, Hawaii) and concluded that this texture might be a relatively common feature of basaltic volcanism. Fluvial transport supports a higher number of grain collisions leading to intense abrasion and, thus, produces rounded grains (Bjorlykke, 2010). Hence, the amount of rounded mineral grains in the samples will indicate the proportion of this alternative transport mechanism. The lack of rounded grains in the studied samples indicates that none of the particles were significantly transported by fluvial processes as the presence of channels in Ka'u Desert initially gave reason to suggest. These volcanic particles, primarily glass shards, are easily abraded particularly in pyroclastic flows such as base surges (McPhie *et al.*, 1990).

The overall spectral shape of the terrestrial spectra reflects a basaltic composition, dominated by olivine and pyroxene. The mafic composition of the sand is fairly similar to that of Martian dark aeolian dunes, which are dominated by pyroxene followed by olivine (Tirsch *et al.*, 2011). Both mafic rock-forming minerals are commonly constituents in basaltic volcanic rock and ash. The sources of the Ka'u Desert dune sands are ash and tephra erupted from the volcanoes in the direct vicinity and lava disintegration particles (e.g. Stearns, 1925; Powers, 1948; Gooding, 1982; Edgett and Lancaster, 1993). A similar volcanic ash origin for Martian dunes has been suggested by Tirsch *et al.* (2011) who found mineralogical similarities and the morphological evidence for layers of volcanic ash being the source of the dark material on Mars. The correlation in mineralogical composition of terrestrial and Martian material suggests a similar volcanic origin. Most samples (DS1, DS3, and DS6) show no indication of hydration of alteration. Two of the terrestrial spectra (DS2 and DS10) show water-associated bands at 1.9 and 2.21 μm that are still visible in the spectra of the dried samples measured under vacuum conditions. Thus, these features indicate juvenile water in the glass particles, i.e. dissolved OH and H₂O in the melt or in some cases meteoric water by glass hydration. The latter case may be true for those glass particles that are less fresh and show an early stage of recrystallization (i.e. sample DS10; cf. Table II). These findings confirm the results of our microprobe analysis, which arrives at a water content of the volcanic glass particles of 5.3 to 5.7 wt. % (cf. Table I). Our results are consistent with the findings of Seelos *et al.* (2010) and Chemtob *et al.* (2010) who detected

opaline (amorphous, hydrated) silica in different samples of lava flows, ash deposits, and solfatara incrustations collected in Ka'u Desert. Furthermore, the spectral shape of sample DS10 almost perfectly fits the spectral shape of altered olivine presented by Orofino *et al.* (2006) (Figure 10) who analyzed altered olivine found in the German region Eifel. Both spectra show clearly absorption bands at 1.9 and around 2.21 μm , which are caused by H₂O and OH in the material.

The particle source identification is somewhat limited. The dominance of glass particles and its well-sorted grain size in sample DS3 clearly indicates a primary deposition from prehistoric phreatomagmatic eruptions at Kilauea. Hence, it represents a primary volcanic sediment (i.e. ash) which may have been slightly modified by aeolian processes. In contrast, the correlation of lithic fragments to their source regions is less certain. In principle, there are three possible sources for lithic fragments: They are derived from (1) aeolian transport and redeposition of weathered lava-flow particles, (2) fluvial channels, and (3) airfall: direct deposition of an ash cloud where lithic fragments represent accidental clasts produced during volcanic eruptions due to vent clearing and widening. Placing the sample into context rules out source 3 because while airfall could result in sedimentary layers, we saw layers that were fairly uniform in thickness, which would not typically be the case from multiple phreatomagmatic eruptions that varied in intensity. Also, the sample is well sorted, even at depth. While it is possible that airfall deposits could also be well-sorted, this is generally not the case. Again, different eruptions would produce deposits where the mean particle size was different. We did not observe that in our samples. Source 2 can be neglected because there were no fluvial channels nearby to the climbing dune. Instead, there were climbing and falling dunes covering the local lava flows. The closest lava flow was erupted in 1984 and it was covered in sand, which emphasizes the importance in aeolian transport (source 1).

Our bulk grain size analyses of Hawaiian basaltic dune sands shows values in the size range fine to medium sand (0.21 and 0.27 mm). One exclusion is sample DS2 (climbing dune, top layer) which consists of coarse sand (up to 2 mm). The mean grain sizes of the Martian basaltic dune materials range between medium and coarse sand [in this study: 0.39–0.9 mm (Tirsch, 2009)]. Thus, the grains sizes of the terrestrial and Martian sands are comparable. In Ka'u Desert the dune material experiences relative short transport distances from the source (i.e. Kilauea) to the bedforms (between 6.2 and 17.4 km). The fine sand glass particles in sample DS3 (climbing dune, vitric layer at 2.9 m depth) are likely to be

deposited *in situ* and were not transported by saltation for long distances, as inferred from their angular grain shape [saltation results in subrounded grain shapes (e.g. Pye and Tsoar, 1990)]. However, mineral grains in that sample are subrounded and seem to be mixed with the vitric material after aeolian transport. The medium and coarse sand materials (samples DS1, DS2, DS6, DS10, cf. Figure 5) seem to be transported primarily by saltation which is inferred from their grain shape and grain size, which is typical for saltation. These medium and coarse sand materials form the bulk of the dune bodies found in Ka'u Desert. The deposition as dune is again a typical indicator for aeolian transport. Aeolian sand transport led to the formation of the dune bodies often nearby topographic obstacles acting as sand traps. The transport distances in Ka'u Desert are relative small (up to ~18 km) compared to Mars. The exemplary Martian deposits were selected by their geographic locations at various distances to volcanic provinces. For our Martian examples we have transport distances between ~410 and ~2260 km, if we assume the material sources to be the nearest volcanic edifice (cf. Figure 3). However, on Mars there are two different cases that could explain the great distance from the ultimate source (i.e. the volcano) to deposition (i.e. the dune), which must not correspond to the effective transport distance in every instance. In the first case, we see dark dunes in craters comprising an obvious local sediment source. Tirsch *et al.* (2011) report that the dark aeolian sediment seem to be almost globally deposited in subsurface layers, which are exposed at crater walls and at crater floors in many places. The volcanic ash material emerges locally from these exposed dark source layers and builds dunes nearby the source preferentially on the floors of impact craters where the sediment is trapped. Hence, in some cases transport distances on Mars are actually relative short (in the order of tens of kilometers, from crater wall to dune) and become comparable to Earth. In a second case, we have dunes at places where no local source can be recognized. Here, the long distance from volcano to dune can be explained by the fact that aeolian transport can reach much higher and longer trajectory pathways compared to Earth. Due to the lower atmospheric pressure and density on Mars, threshold friction velocities are 10 times higher than on Earth (Greeley *et al.*, 1980; Edgett and Christensen, 1991). This means that higher wind speeds are required to move similar-sized grains on Mars than on Earth. In a thinner atmosphere, the greater initial grain velocity coupled with the lower gravity causes the grains' saltation path to lengthen. Thus, the path lengths of grains of up to 210 μm in diameter begin to approach infinity (Edgett and Malin, 2002). Because of the higher surface friction velocities needed to move particles at low atmospheric pressures and a lower gravity, larger grains can become suspended on Mars than on Earth. Although it takes stronger winds to saltate particles on Mars and the saltating particles are coarser-grained than on Earth, trajectories are longer and flatter, varying with temperature and atmospheric conditions (e.g. White, 1979; Iversen and White, 1982; Greeley *et al.*, 1999; Fenton, 2005). Thus, although not relevant for every dark deposit, extreme long aeolian transport distances are possible due to the specific physics of particle motion on Mars.

The strong spectral correlation between Martian dark aeolian sediments and terrestrial basaltic sands encourages the interpretation that the Martian dune material has a similar composition as the terrestrial basaltic sands. The confirmation of a similar glass content of the Martian sands is somewhat difficult. Basaltic glass has a spectral signature similar to that of pyroxene showing excitational bands near 1.1 μm and 1.9 μm (e.g. Minitti *et al.*, 2002; Bishop *et al.*, 2003). The lower the degree of crystallinity the lower the expression of these absorptions (Minitti *et al.*, 2002). Since we have no information on the

degree of crystallinity of the Martian volcanic glasses, we cannot estimate the influence of volcanic glass on the Martian spectra. However, a first hint can be deduced from comparisons between experimental and observed basalt spectra done by Minitti *et al.* (2002) that show that VIS/NIR spectra of oxidized, 55% crystallized fine particle basalt best fit to spectra of dark regions on Mars. Following these results, glasses in the Martian dark sands might be partially recrystallized and hence could influence the Martian spectra perceptibly. Nevertheless, following our analysis we can only confirm the constituents olivine and HCP and LCP but cannot determine the exact amount of volcanic glass in the Martian sediments. However, if there is indeed an analogy in origin between terrestrial and Martian sands, we can suppose that the Martian dark sediments might have a similar high content of volcanic glass as the terrestrial basaltic sands. Further components such as plagioclase and dust can only be modeled for the Martian sands (cf. Tirsch *et al.*, 2011). We do see similarities in the spectra from Earth and Mars but we cannot confirm a 100% correlation. If there is volcanic glass in the Martian sands, it may not comprise juvenile water or hydration features since we do not see any water associated bands in the Martian spectra (e.g. Tirsch *et al.*, 2011). Hence, Martian dune sands seem to be unweathered, which is the main difference between both materials revealed yet. Prospectively we can assume, that the detection of absorptions bands related to H₂O and OH in the dark Martian sediment spectra will be a further step to finally prove the volcanic origin of these basaltic sands, but only if we can prove that the water is associated to water in volcanic glass particles.

There are some limitations of our methodology that need to be mentioned here. The spectral measurements were not accomplished under Martian conditions, but under terrestrial ambient atmosphere and vacuum conditions. This has to be considered when comparing the spectra. Additionally, terrestrial weather is much more humid than Martian climatic conditions, making direct comparison difficult. The comparatively humid conditions in Ka'u Desert might be the main reason for differing weathering stages of the basaltic sands on Mars and Earth. Thus, the similar initial conditions of the sediments have to be the focus, and the aqueous alteration observed has to be regarded as a result of terrestrial conditions.

Conclusions

The aim of this study was to characterize sand samples collected in Ka'u Desert, to compare these volcanic sands with spectra of dark aeolian sediments on Mars as a way of determining the source of the Martian dunes. We conclude that the Ka'u Desert sands were derived from airfall ashes from phreatomagmatic eruptions of Kilauea and reworked lava. Grain shapes dominated by subsounded to subangular forms indicate transport by aeolian rather than fluvial processes, which is also expressed by the high number of aeolian bedforms. Compositionally, the Ka'u Desert dune samples are dominated by olivine, pyroxene, plagioclase, and glasses resulting from the volcanic source of these aeolian sediments. This composition correlates very well with the composition of Martian dark aeolian sediments, which are dominated by pyroxene and olivine (Tirsch *et al.*, 2011). We conclude that this correlation can be seen as a further indication for a volcanic origin of the Martian dark sediments similar to the origin of the basaltic sands of Hawaii. Furthermore, we suggest that, analogously to the terrestrial volcanic sands, a similar high amount of volcanic glass can be expected in the Martian sands. Unlike the Martian dark aeolian sediments, the spectra of the terrestrial basaltic sands show indications of hydration and slight alteration which

is presumably related to the comparatively humid conditions on Earth.

Acknowledgments—This research and fieldwork has been supported by NASA's Mars Fundamental Research Program, Grant NNX09AC27G, funds from the George F. Becker Endowment at the Smithsonian Institution, and by the Helmholtz Association through the research alliance 'Planetary Evolution and Life'. The authors thank Daniel Spengler (Helmholtz Centre Potsdam GFZ German Research Center for Geosciences, Potsdam) for valuable assistance with the ASD spectral measurements and Mirjam Langhans (DLR Berlin/INAF-IASF Rome) for priceless field support. The authors acknowledge the reviews of Janice Bishop and Vincenzo Orofino that significantly improved this paper.

References

- Anderson JH, Wickersheim KA. 1964. Near infrared characterization of water and hydroxyl groups on silica surfaces. *Surface Science* **2**: 252–260.
- Baird AK, Clark BC. 1981. On the original igneous source of Martian fines. *Icarus* **45**: 113–123. DOI: 10.1016/0019-1035(81)90009-9
- Bandfield JL. 2000. A global view of Martian surface compositions from MGS-TES. *Science* **287**: 1626–1630.
- Bandfield JL. 2002. Global mineral distributions on Mars. *Journal of Geophysical Research* **107**: E6, 5042. DOI: 10.1029/2001JE001510
- Baratoux D, Mangold N, Arnalds O, Grégoire, Platvoet B, Badinzeff JM, Pinet P. 2007. *Formation, Transport and Mineralogical Evolution of Basaltic Sands on Earth and Mars*, Lunar and Planetary Institute Contribution 1353. Lunar and Planetary Institute: Houston, TX; 3048.
- Basilevsky A, Yakovlev O, Fisenko A, Semjonova L, Semenova A, Barsukova L, Roshchina I, Galuzinskaya A, Stroganov I, Moroz L, Pieters C, Hiroi T, Zinovieva N. 2000. Simulation of impact melting effect on spectral properties of Martian surface: implications for polar deposits. *Geochemistry International* **38**(Suppl. 3): 390–403.
- Bell JF III, Morris RV, Adams JB. 1993. Thermally altered palagonitic tephra: a spectral and process analog to the soil and dust of Mars. *Journal of Geophysical Research* **98**: 3373–3385.
- Bishop JL, Pieters CM. 1995. Low-temperature and low atmospheric pressure infrared reflectance spectroscopy of Mars soil analog materials. *Journal of Geophysical Research* **100**: 5369–5379.
- Bishop JL, Pieters CM, Edwards JO. 1994. Infrared spectroscopic analyses on the nature of water in montmorillonite. *Clays and Clay Minerals* **42**: 701–715.
- Bishop JL, Pieters CM, Burns RG, Edwards JO, Mancinelli RL, Froeschl H. 1995. Reflectance spectroscopy of ferric sulfate-bearing montmorillonites as Mars soil analog materials. *Icarus* **117**: 101–119.
- Bishop JL, Miniti ME, Lane MD, Weitz CM. 2003. *The Influence of Glassy Coatings on Volcanic Rocks from Mauna Iki, Hawaii and Applications to Rocks on Mars*, Lunar and Planetary Institute Science Conference Abstracts 34. Lunar and Planetary Institute: Houston, TX; 1516.
- Bishop JL, Schiffman P, Murad E, Dyar MD, Drief A, Lane MD. 2007. Characterization of alteration products in tephra from Haleakala, Maui: a visible-infrared spectroscopy, Mossbauer Spectroscopy, XRD, EMPA and TEM study. *Clays and Clay Minerals* **55**: 1–17.
- Bjorlykke K. 2010. *Petroleum Geology – From Sedimentary Environments to Rock Physics*. Springer: Berlin.
- Bourke MC, Edgett KS, Cantor BA. 2008. Recent eolian dune change on Mars. *Geomorphology* **94**(1–2): 247–255.
- Bullock M, Moore J. 2004. Aqueous alteration of Mars-analog rocks under an acidic atmosphere. *Geophysical Research Letters* **31**: L14701. DOI: 10.1029/2004GL019980
- Burns RG. 1993. *Mineralogical Applications of Crystal Field Theory*. Cambridge University Press: Cambridge.
- Chakroun A, Miskovsky J-C, Zaghib-Turki D. 2009. Quartz grain surface features in environmental determination of aeolian Quaternary deposits in northeast Tunisia. *Mineralogical Magazine* **73**: 607–614.
- Chemtob SM, Jolliff BK, Rossman GR, Eiler JM, Arvidson RE. 2010. Silica coatings in the Ka'u Desert, Hawaii, a Mars analog terrain: a micromorphological, spectral, chemical, and isotopic study. *Journal of Geophysical Research (Planets)* **115**: E04001. DOI: 10.1029/2009JE003473
- Christensen P, Bandfield J, Smith DE, Hamilton V, Clark R. 2000. Identification of a basaltic component on the Martian surface from thermal emission spectrometer data. *Journal of Geophysical Research* **105**(E4): 9609–9621.
- Christiansen RL. 1979. Explosive Eruption of Kilauea Volcano in 1790, Hawaii Symposium on Intraplate Volcanism and Submarine Volcanism, Hilo, Hawaii; 158.
- Clark RN, King TVV, Klejwa M, Swayze GA, Vergo N. 1990. High spectral resolution reflectance spectroscopy of minerals. *Journal of Geophysical Research* **95**(B8): 12653–12680.
- Cloutis EA. 2004. *Spectral reflectance properties of some basaltic weathering products*, Lunar and Planetary Institute Science Conference Abstracts 35. Lunar and Planetary Institute: Houston, TX; 1265.
- Cloutis EA, Gaffey MJ. 1991. Pyroxene spectroscopy revisited: spectral-compositional correlations and relationships to geothermometry. *Journal of Geophysical Research* **96**: 22809–22826.
- Cloutis EA, Gaffey MJ, Jackowski T, Reed K. 1986. Calibrations of phase abundance, composition, and particle size distribution for olivine-orthopyroxene mixtures from reflectance spectra. *Journal of Geophysical Research* **91**(B11): 11641–11653.
- Craddock RA, Howard AD, Tirsch D, Zimbleman JR. 2010. *Preliminary Analyses of Basaltic Dunes in the Ka'u Desert, Hawaii and Implications for Understanding Dunes on Mars*, Lunar and Planetary Institute Science Conference Abstracts 41. Lunar and Planetary Institute: Houston, TX; 2164.
- Decker RW, Christiansen RL. 1984. Explosive eruptions of Kilauea volcano, Hawaii. In *Explosive Volcanism: Inception, Evolution, and Hazards*. National Academic Press: Washington, DC; 122–132.
- Dzurisin D, Lockwood JP, Casadevall TJ, Rubin M. 1995. The Uwekahuna ash member of the Puna Basalt: product of violent phreatomagmatic eruptions at Kilauea volcano, Hawaii between 2800 and 2100 14C years ago. *Journal of Volcanology and Geothermal Research* **66**: 163–184.
- Easton RM. 1987. *Stratigraphy of Kilauea Volcano*, US Geological Survey Professional Paper 1350. US Geological Survey: Reston, VA; 243–260.
- Edgett KS, Blumberg DG. 1994. Star and linear dunes on Mars. *Icarus* **112**: 448–464. DOI: 10.1006/icar.1994.1197
- Edgett KS, Christensen PR. 1991. The particle size of Martian aeolian dunes. *Journal of Geophysical Research* **96**(E5): 22762–22776.
- Edgett KS, Christensen PR. 1994. Mars aeolian sand: regional variations among dark-hued crater floor features. *Journal of Geophysical Research* **99**(E1): 1997–2018.
- Edgett KS, Lancaster N. 1993. Volcaniclastic aeolian dunes: terrestrial examples and application to Martian sands. *Journal of Arid Environments* **25**: 271–297.
- Edgett KS, Malin MC. 2002. Martian sedimentary rock stratigraphy: outcrops and interbedded craters of northwest Sinus Meridiani and southwest Arabia Terra. *Geophysical Research Letters* **29**(24): 2179. DOI: 10.1029/2002GL016515
- Elias T, Sutton AJ, Stokes JB, Casadevall TJ. 1998. *Sulfur Dioxide Emissions Rates of Kilauea Volcano, Hawaii, 1979–1997*, US Geological Survey Open File Report 98–462. US Geological Survey: Reston, VA; 41.
- Fenton L. 2005. Potential sand sources for the dune fields in Noachis Terra, Mars. *Journal of Geophysical Research* **110**: E11004. DOI: 10.1029/2005JE002436
- Fenton L, Bandfield J. 2003. Aeolian processes in Proctor Crater on Mars: sedimentary history as analyzed from multiple data sets. *Journal of Geophysical Research* **108**(E12): E06005. DOI: 10.1029/2002JE002015
- Fisher VR. 1963. Bubble-wall texture and its significance. *Journal of Sedimentary Research* **33**(1): 224–227.
- Folk RL. 1978. Angularity and silica coatings of Simpson Desert sand grains, Northern Territory. *Journal of Sedimentary Petrology* **52**: 93–101.
- Froggatt P. 1983. Toward a comprehensive upper Quaternary tephra and ignimbrite stratigraphy in New Zealand using electronmicroprobe analysis of glass shards. *Quaternary Research* **19**: 188–200.
- Giambelluca T, Sanderson M. 1993. The water balance and climate classification. In *Prevailing Trade Winds: Weather and Climate in Hawaii*, Sanderson M (ed.). University of Hawaii Press: Honolulu; 56–72.

- Golden DC, Morris RV, Ming DW, Lauer Jr HV, Yang SR. 1993. Mineralogy of three slightly palagonitized basaltic tephra samples from the summit of Mauna Kea, Hawaii. *Journal of Geophysical Research* **98**: 3401–3411.
- Golombek MP, Cook RA, Economou T, Folkner WM, Haldemann AFC, Kallemeyn PH, Knudsen JM, Manning RM, Moore HJ, Parker TJ, Rieder R, Schofield JT, Smith PH, Vaughan RM. 1997. Overview of the Mars Pathfinder mission and assessment of landing site predictions. *Science* **278**: 1743. DOI: 10.1126/science.278.5344.1743
- Gooding JL. 1982. Petrology of dune sand derived from basalt on the Ka'u Desert, Hawaii. *Journal of Geology* **90**: 97–108.
- Goudie AS, Watson A. 1981. The shape of desert sand dune grains. *Journal of Arid Environments* **4**: 185–190.
- Greeley R, Leach R, White B, Iversen J, Pollack J. 1980. Threshold windspeeds for sand on Mars: wind tunnel simulations. *Geophysical Research Letters* **7**(2): 121–124.
- Greeley R, Kraft M, Sullivan R, Wilson G, Bridges N, Herkenhoff K, Kuzmin RO, Malin M, Ward W. 1999. Aeolian features and processes at the Mars Pathfinder landing site. *Journal of Geophysical Research* **104**: 8573–8584. DOI: 10.1029/98JE02553
- Hamilton V, Morris R, Gruener J, Mertzman S. 2008. Visible, near-infrared, and middle infrared spectroscopy of altered basaltic tephra: spectral signatures of phyllosilicates, sulfates, and other aqueous alteration products with application to the mineralogy of the Columbia Hills of Gusev Crater, Mars. *Journal of Geophysical Research (Planets)* **113**: E12S43. DOI: 10.1029/2007JE003049
- Hausrath EM, Navarre-Stichler AK, Sak PB, Steefel CI, Brantley SL. 2008. Basalt weathering rates on Earth and the duration of liquid water on the plains of Gusev Crater, Mars. *Geology* **36**: 67–70. DOI: 10.1130/G24238A.
- Hayward RK, Mullins KF, Fenton LK, Hare TM, Titus TN, Bourke MC, Colaprete A, Christensen PR. 2007. Mars global digital dune database and initial science results. *Journal of Geophysical Research* **112**: E11007. DOI: 10.1029/2007JE002943
- Iversen J, White B. 1982. Saltation thresholds on Earth, Mars, and Venus. *Sedimentology* **29**: 111–119.
- Juvik SP, Juvik JO (eds). 1998. *Atlas of Hawai'i*, 3rd edn. University of Hawai'i Press: Honolulu.
- Krinsley DR, Greeley R, Pollack JB. 1979. Abrasion of windblown particles on Mars – erosion of quartz and basaltic sand under simulated Martian conditions. *Icarus* **39**: 364–384. DOI: 10.1016/0019-1035(79)90147-7
- Malin MC, Dzuris D, Sharp RP. 1983. Stripping of Keanakaoi tephra on Kilauea Volcano, Hawaii. *Geological Society of America Bulletin* **94**: 1148–1158.
- Mangold N, Poulet F, Mustard JF, Bibring JP, Gondet B, Langevin Y, Ansan V, Masson P, Fassett C, Head JW, Hoffmann H, Neukum G. 2007. Mineralogy of the Nili Fossae region with OMEGA/Mars Express data: 2. Aqueous alteration of the crust. *Journal of Geophysical Research (Planets)* **112**: E08S04. DOI: 10.1029/2006JE002835
- Mangold N, Baratoux D, Arnalds O, Bardintzeff JM, Platvoet B, Grégoire M, Pinet P. 2010a. *Segregation of olivine grains in volcanic sands in Iceland – implications for Mars*. Lunar and Planetary Institute Contribution 1552. Lunar and Planetary Institute: Houston, TX; 47–48.
- Mangold N, Loizeau D, Gaudin A, Ansan V, Michalski J, Poulet F, Bibring JP. 2010b. *Connecting fluvial Landforms and the Stratigraphy of Mawrth Vallis Phyllosilicates: Implications for Chronology and Alteration Processes*, Lunar and Planetary Institute Contribution 1547. Lunar and Planetary Institute: Houston, TX; 40.
- Mastin LG. 1997. Evidence for water influx from a caldera lake during the explosive hydromagmatic eruption of 1790, Kilauea volcano, Hawaii. *Journal of Geophysical Research* **102**: 20093–20109. DOI: 10.1029/97JB01426
- Maturilli A. 2010. All you can measure at the Planetary Emissivity Laboratory (PEL) at DLR, in Berlin, EPSC 2010 abstracts 20–24, September 2010, Rome, Italy.
- McPhie J, Walker GPL, Christiansen RL. 1990. Phreatomagmatic and phreatic fall and surge deposits from explosions at Kilauea volcano, Hawaii, 1790 A.D.: Keanakaoi ash member. *Bulletin Volcanologique* **52**: 334–354.
- Milliken RE, Swayze GA, Arvidson RE, Bishop JL, Clark RN, Ehlmann BL, Green RO, Grotzinger J, Morris RV, Murchie SL, Mustard JF, Weitz CM. 2008. Opaline silica in young deposits on Mars. *Geology* **36**: 847–850. DOI: 10.1130/G24967A.1
- Minitti ME, Mustard JF, Rutherford MJ. 2002. The effects of glass content and oxidation on the spectra of SNC-like basalts: application to Mars remote sensing. *Journal of Geophysical Research* **107**(6): 1–16.
- Minitti ME, Weitz CM, Lane MD, Bishop JL. 2007. Morphology, chemistry, and spectral properties of Hawaiian rock coatings and implications for Mars. *Journal of Geophysical Research (Planets)* **112**: E05015. DOI: 10.1029/2006JE002839
- Morimoto N. 1989. Nomenclature of pyroxenes. *Canadian Mineralogist* **27**: 143–156
- Moroz LV, Basilevsky AT, Hiroi T, Rout SS, Baither D, van der Bogert CH, Yakovlev OI, Fisenko AV, Semjonova LF, Rusakov VS, Khramov DA, Zinovieva NG, Arnold G, Pieters CM. 2009. Spectral properties of simulated impact glasses produced from Martian soil analogue JSC Mars-1. *Icarus* **202**: 336–353. DOI: 10.1016/j.icarus.2009.02.007
- Morris RV, Lauer Jr HV, Lawson CA, Gibson Jr EK, Nace GA, Stewart C. 1985. Spectral and other physicochemical properties of submicron powders of hematite (α -Fe₂O₃), maghemite (γ -Fe₂O₃), magnetite (Fe₃O₄), goethite (α -FeOOH), and lepidocrocite (γ -FeOOH). *Journal of Geophysical Research* **90**: 3126–3144.
- Morris RV, Gooding JL, Lauer Jr HV, Singer RB. 1990. Origins of Mars-like spectral and magnetic properties of a Hawaiian palagonitic soil. *Journal of Geophysical Research* **95**: 14427–14434.
- Orofino V, Politi R, Blanco A, Fonti S. 2006. Diffuse reflectance of altered olivine grains: remote sensing detection and implications for Mars studies. *Planetary and Space Science* **54**: 784–793. DOI: 10.1016/j.pss.2006.04.009
- Platz T, Cronin SJ, Smith IEM, Turner MB, Stewart RB. 2007. Improving the reliability of microprobe-based analyses of andesitic glasses for tephra correlation. *The Holocene* **17**: 573–583.
- Powers HA. 1916. Explosive ejection of Kilauea. *American Journal of Science* **4**: 227–244.
- Powers HA. 1948. A chronology of the explosive eruptions of Kilauea. *Pacific Science* **2**: 278–292.
- Pye K, Tsoar H. 1990. *Aeolian Sand and Sand Dunes*. Unwin Hyman: London.
- Rogers D, Christensen P. 2003. Age relationship of basaltic and andesitic surface compositions on Mars: analysis of high-resolution TES observations of the northern hemisphere. *Journal of Geophysical Research* **108**(E4): 5030. DOI: 10.1029/2002JE001913
- Ruff SW, Christensen P. 2002. Bright and dark regions on Mars: particle size and mineralogical characteristics based on thermal emission spectrometer data. *Journal of Geophysical Research* **107**(E12): 5127. DOI: 10.1029/2001JE001580
- Schiffman P, Spero HJ, Southard RJ, Swanson DA. 2000. Controls on palagonitization versus pedogenic weathering of basaltic tephra: evidence from the consolidation and geochemistry of the Keanakao'i Ash Member, Kilauea volcano. *Geochemistry, Geophysics, Geosystems* **1**: 2000GC000,068.
- Schiffman P, Southard RJ, Eberl DD, Bishop JL. 2002. Distinguishing palagonitized from pedogenically-altered basaltic Hawaii tephra: mineralogical and geochemical criteria. In *Volcano-Ice Interaction on Earth and Mars*, Smellie SL, Chapman MG (eds), Geological Society of London, Special Publications. Geological Society: London; 393–405.
- Schiffman P, Zierenberg R, Marks N, Bishop JL, Dyar MD. 2006. Acid-fog deposition at Kilauea volcano: a possible mechanism for the formation of siliceous-sulfate rock coatings on Mars. *Geology* **34**: 921–924. DOI: 10.1130/G22620A.1
- Schultz P, Mustard J. 2004. Impact melts and glasses on Mars. *Journal of Geophysical Research* **109**: E01001. DOI: 10.1029/2002JE002025
- Seelos KD, Arvidson RE, Jolliff BL, Chemtob SM, Morris RV, Ming DW, Swayze GA. 2010. Silica in a Mars analog environment: Ka'u Desert, Kilauea Volcano, Hawaii. *Journal of Geophysical Research (Planets)* **115**: E00D15. DOI: 10.1029/2009JE003347
- Smalley IJ, Krinsley DH. 1979. Eolian sedimentation on Earth and Mars – some comparisons. *Icarus* **40**: 276–288. DOI: 10.1016/0019-1035(79)90072-1
- Squyres SW, Knoll AH. 2005. Sedimentary rocks at Meridiani Planum: origin, diagenesis, and implications for life on Mars. *Earth and Planetary Science Letters* **240**: 1–10. DOI: 10.1016/j.epsl.2005.09.038

- Squyres SW, Arvidson RE, Bell JF, Brückner J, Cabrol NA, Calvin W, Carr MH, Christensen PR, Clark BC, Crumpler L, Des Marais DJ, d'Uston C, Economou T, Farmer J, Farr W, Folkner W, Golombek M, Gorevan S, Grant JA, Greeley R, Grotzinger J, Haskin L, Herkenhoff KE, Hviid S, Johnson J, Klingelhöfer G, Knoll AH, Landis G, Lemmon M, Li R, Madsen MB, Malin MC, McLennan SM, McSween HY, Ming DW, Moersch J, Morris RV, Parker T, Rice JW, Richter L, Rieder R, Sims M, Smith M, Smith P, Soderblom LA, Sullivan R, Wänke H, Wdowiak T, Wolff M, Yen A. 2004. The Opportunity Rover's Athena Science Investigation at Meridiani Planum, Mars. *Science* **306**: 1698–1703.
- Squyres SW, Aharonson O, Clark BC, Cohen BA, Crumpler L, de Souza PA, Farrand WH, Gellert R, Grant J, Grotzinger JP, Haldemann AFC, Johnson JR, Klingelhöfer G, Lewis KW, Li R, McCoy T, McEwen AS, McSween HY, Ming DW, Moore JM, Morris RV, Parker TJ, Rice JW, Ruff S, Schmidt M, Schröder C, Soderblom LA, Yen A. 2007. Pyroclastic activity at Home Plate in Gusev Crater, Mars. *Science* **316**: 738–742. DOI. 10.1126/science.1139045
- Squyres SW, Arvidson RE, Ruff S, Gellert R, Morris RV, Ming DW, Crumpler L, Farmer JD, Des Marais DJ, Yen A, McLennan SM, Calvin W, Bell JF, Clark BC, Wang A, McCoy TJ, Schmidt ME, de Souza PA. 2008. Detection of silica-rich deposits on Mars. *Science* **320**: 1063–1067. DOI. 10.1126/science.1155429
- Stearns H. 1925. The explosive phase of Kilauea Volcano, Hawaii, in 1924. *Bulletin Volcanologique* **2**(2): 193–208.
- Stearns HT, MacDonald GA. 1946. *Geology and groundwater resources of the island of Hawaii*. Hawaii Division of Hydrography, Bulletin 9. Hawaii Division of Hydrography: Honolulu; 363.
- Sunshine JM, Pieters CM. 1998. Determining the composition of olivine from reflectance spectroscopy. *Journal of Geophysical Research* **103**: 13675–13688.
- Tirsch D. 2009. Dark Dunes on Mars – Analyses on Origin, Morphology and Mineralogical Composition of the Dark Material in Martian Craters, PhD Thesis, Freie Universität Berlin. http://www.diss.fu-berlin.de/diss/receive/FUDISS_thesis_000000008848
- Tirsch D, Jaumann R, Poulet F, Matz KD, Bibring J-P, Neukum G. 2008. A global view on the mineralogical composition of dark dunes on Mars. Lunar and Planetary Institute Science Contribution 1391. Lunar and Planetary Institute: Houston, TX; 1693.
- Tirsch D, Jaumann R, Pacifici A, Poulet F. 2011. Dark aeolian sediments in Martian craters: composition and sources. *Journal of Geophysical Research (Planets)* **116**: E03002. DOI. 10.1029/2009JE003562
- White B. 1979. Soil transport by winds on Mars. *Journal of Geophysical Research* **84**: 4643–4651. DOI. 10.1029/JB084iB09p04643
- Wilson D, Elias T, Orr T, Patrick M, Sutton J, Swanson DA. 2008. Small explosion from new vent at Kilauea's summit. *Eos* **89**(22): 203. DOI. 10.1029/2008EO220003
- Wrobel KE, Schultz PH. 2006. The Generation and Distribution of Martian Impact Melt/Glass: A Computational Study with Implications for the Nature of Dark Surface Materials, 37th Annual Lunar and Planetary Science Conference, Lunar and Planetary Institute Technical Report 37. Lunar and Planetary Institute: Houston, TX; 2386.
- Wrobel KE, Schultz PH. 2007. *The Significant Contribution of Impact Glass to the Martian Surface Record*, Lunar and Planetary Institute Science Contribution 1353. Lunar and Planetary Institute: Houston, TX; 3093.
- Wyatt MB, McSween HY, Moersch JE, Christensen PR. 2003. Analysis of surface compositions in the Oxia Palus region on Mars from Mars Global Surveyor Thermal Emission Spectrometer Observations. *Journal of Geophysical Research (Planets)* **108**(E9): 5107. DOI. 10.1029/2002JE001986
- Zablocki CJ, Tilling RI, Peterson DW, Christiansen RL, Keller GV, Murray JC. 1974. A deep research drill hole at the summit of an active volcano, Kilauea, Hawaii. *Geophysical Research Letters* **1**: 323–326. DOI. 10.1029/GL001i007p00323